Received: 31 March 2024; Accepted: 1 July 2024; Published: 12 July 2024; Corrected and Typeset: 1 September 2024

of siderophores, effectively cutting off iron supply to pathogens [19, 20]. FP6, a biocontrol strain inhibiting the fungal pathogen , lost almost all its inhibitory activity against . after $FeCl_3$ supplementation, highlighting the role of iron competition as the main mechanism for pathogen control [20]. Extensive literature documents the variety and functionality of siderophores produced by spp. [21, 22], as well as their contributions to disease prevention [23]. Pyoverdines, a diverse class of non-ribosomal peptides that possess the most complex chemical structures among siderophores, have been extensively studied, and over 50 structurally distinct pyoverdines have been identified [24]. The structural complexity of siderophores is noteworthy for its diversity, exhibiting remarkable variation even within a single bacterial strain [24]. Here we focused on spp. siderophores due to their great structural diversity and substantial potential for biological control applications [25, 26]. Furthermore, pyoverdines are highly specific. Their uptake requires very specific receptors, driving the same molecule to promote or inhibit bacterial strains depending on their ability to use it [27]. Thus, siderophore-mediated competition for iron shapes ecological interactions between microorganisms [28]. In the multispecies rhizosphere microbiome, these interactions may ultimately affect the performance and health of plant hosts [29, 30].

Although many studies have approached the importance of

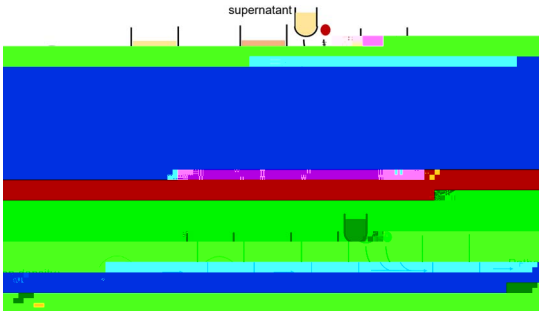

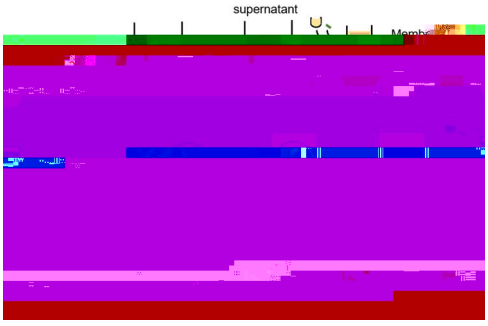

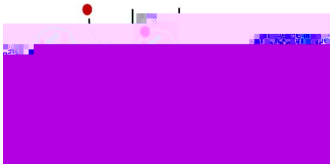

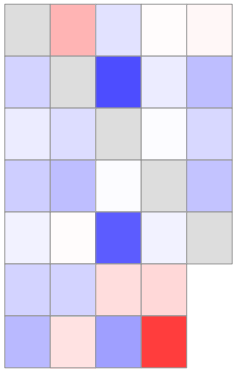

the pathogen . . Extensive research has illustrated the pivotal role of siderophores produced by biocontrol agents in the suppression of pathogenic bacteria, the level of suppression positively correlating with increased siderophore production [31, 46]. Consistent with these findings, we observed that the production of competitive siderophores by strains

pathogen could stem from the constraints on growth antagonism induced by limited iron availability.

Iron deficiency dramatically affects the utilization of metabolic pathways related to iron, favoring iron-independent pathways while curtailing iron-dependent ones [59

Determining the siderophore production of consortium members and bacterial consortia

Siderophore production in bacterial strains and consortia was measured by chrome azurol S (CAS) assays, which gauge the intensity of siderophores chelating ferric ions based on the resulting color change in the reaction mixture [67]. All strains and bacterial consortia were cultured (30°C, 48 h, 170 r.p.m.) in MKB medium and iron-rich MKB medium (MKB + Fe), respectively. Cell-free supernatants were obtained by centrifugation (6000 r.p.m. for 10 min) and subsequent filtration using a 0.22-μm filter and then assayed for siderophore production by a modified version of the universal CAS assay developed by Schwyn and Neilands [67]. Briefly, 100 μl of each cell-free supernatant (three biological replicates for all 49 bacterial consortia) or fresh medium as a control, was combined with 100 μl of the CAS assay solution (containing 1.5×10^{-3} mM $FeCl_3 \cdot 6H_2O$, 6×10^{-1} mM adecyltrimethylammonium bromide, 4.307 g anhydrous piperazine, and 1.5×10^{-1} mM CAS) in a 96-well microplate. Following 1 h of static cultivation at room temperature, the optical density at 630 nm (OD_{630}) of cell-free supernatant (A) and the uninoculated medium control (Ar) were measured using a spectrophotometer (SpectraMax M5, Sunnyvale, CA, USA). Deferoxamine B siderophore was utilized as the standard to create standard curves for assessing siderophore production in both strains and microbial communities. Employing the observable color change of the CAS solution upon siderophore presence, diverse dilutions of deferoxamine B siderophore, in combination with OD_{630} measurements, were pivotal in constructing these standard curves. Siderophore concentration was normalized as deferoxamine (DFO) equivalent and expressed as $\log_{10}$DFO. To be noted, the siderophore concentration of the supernatant collected under iron-limited conditions required dilution with sterile water due to saturation in the assay.

Determining the phloroglucinol production and antibiotic gene expression of consortium members under different iron conditions

Phloroglucinol (PG), an intermediate product of DAPG [68, 69], was quantified in the supernatant using a method modified from a previous study [70]. Seven strains were cultured in iron-rich and iron-limited media for 48 h, with each treatment carried out in triplicate. Cell-free supernatants were collected as mentioned above. To each sample (75 μl of supernatant), 25 μl of HCl was added. Following this, 100 μl of cinnamaldehyde–HCl reagent, comprising 0.2% 4-hydroxy-3-methoxy-cinnamaldehyde in HCl:ethanol (1:3, v/v), was introduced to the solution, resulting in a pink coloration in samples containing PG. The colorimetric reaction was allowed to proceed for 2 h, after which the absorbance was measured at 550 nm. The absolute concentration of PG was subsequently determined by referencing a standard curve constructed from varying concentrations of PG standards.

To determine the effect of iron deficiency on antibiotic gene expression, the expression of the *D* gene was assessed under different iron conditions by RT–qPCR. Seven strains were cultured in iron-rich and iron-limited MKB media for 48 h. The total RNA of the bacteria was extracted according to the protocol of the Bacterial RNA Kit (R6950, Omega, USA). The concentration and purity of RNA were determined using a NanoDrop 1000 spectrophotometer (Thermo Scientific, Waltham, MA, USA), with A260/A280 and A260/230 ratio values of around 2 considered adequate for inclusion in the study. cDNA was synthesized with the HiScript® II Q RT SuperMix for qPCR (+gDNA wiper) Kit (Vazyme, China). For RT–qPCR analysis, two primers specific to the *D* gene were used: B2BF (5′-ACC CAC CGC AGC ATC GTT TAT GAGC-3′

supernatants from 49 consortia were collected as described above (Fig. 1A and B). The following three treatments were set up to distinguish siderophore-mediated effects from other metabolite-mediated effects [33]. (i) Iron-limited: 20 μl of cell-free supernatant collected under iron-limited conditions was added to 178 μl of MKB medium. This supernatant contained total metabolites pTf5.98629467.9(m).to 178

sound relationships were considered. All data analyses were performed using R version 4.1.0.

A d t

This research was funded by the National Natural Science Foundation of China (42090060, 42325704, 42277113, and 42107140), the Fundamental Research Funds for the Central Universities (KYT2024001), the Natural Science Foundation of Jiangsu Province (BK20230102), the Jiangsu Agricultural Science and Technology Innovation Fund (CX(22)1004, SCX(24)3511) and the Jiangsu Carbon Peak & Carbon Neutrality Science and Technology Innovation Special Fund (BE2022423).

A t . t t .

Z.W., Y.X., and Q.S.: conceptualization and project administration. Z.S., S.Gu, and Z.W.: methodology, software, formal analysis, visualization, and writing original draft. X.Z., J.X., T.Y., S.Guo, and Z.W.: resources, investigation, and data curation. T.P., A.J., Z.W., and T.Y.: writing – review and editing.

Da a a a t

The data for this article are available in the article or in its supplementary material.

C t t t

The authors declare no conflict of interest.

t a da a

Supplementary data are available at *H* online.

.

1. References
2. Wang Z, Luo W, Cheng S. . – a soil borne hidden enemy of plants: research development in management strategies, their action mechanism and challenges. *F* . 2023;14:1141902
3. An Y, Zhang M. Advances in understanding dynamic host-microbe interactions during infection and their implications for crop disease resistance. *C* . 2024;1:100014
4. Ahmed W, Yang J, Tan Y. . , a deadly pathogen: revisiting the bacterial wilt biocontrol practices in tobacco and other Solanaceae. . 2022;21:100479
5. Jangir M, Pathak R, Sharma S. . Biocontrol mechanisms of *B* sp., isolated from tomato rhizosphere, against *F* f. sp. . *B C* . 2018;123:60–70
6. Trivedi P, Leach JE, Tringe SG. . Plant–microbiome interactions: from community assembly to plant health. . 2020;18:607–21
7. Hunjan MS, Thakur A, Singh PP. Identification and characterization of strains effective against pv. causing bacterial blight of rice in Punjab, India. *J A* . 2017;9:253–61
8. Barahona E, Navazo A, Garrido-Sanz D. . - F113 can produce a second flagellar apparatus, which is important for plant root colonization. *F* . 2016;7:1471
9. Backer R, Rokem JS, Ilangumaran G. . Plant growth-promoting rhizobacteria: context, mechanisms of action, and roadmap to commercialization of biostimulants for sustainable agriculture. *F* . 2018;9:1473
10. Köhl J, Kolnaar R, Ravensberg WJ. Mode of action of microbial biological control agents against plant diseases: relevance beyond efficacy. *F* . 2019;10:845
11. Xu Z, Wang M, Du J. . Isolation of *B* sp. HQB-1, a promising biocontrol bacteria to protect banana against *F* wilt through phenazine-1-carboxylic acid secretion. *F* . 2020;11:605152
12. Jung BK, Hong S-J, Park G-S. . Isolation of *B* - JBK9 with plant growth-promoting activity while producing pyrrolnitrin antagonistic to plant fungal diseases. *A B C* . 2018;61:173–80
13. Feng S, Jin L, Tang S. . Combination of rhizosphere bacteria isolated from resistant potato plants for biocontrol of potato late blight. . 2022;78:166–76
14. Gu S, Wei Z, Shao Z. . Competition for iron drives phytopathogen control by natural rhizosphere microbiomes. . 2020;5:1002–10
15. Wei Z, Yang T, Friman VP. . Trophic network architecture of root-associated bacterial communities determines pathogen invasion and plant health. *C* . 2015;6:8413
16. Andrews SC, Robinson AK, Rodríguez-Quiñones F. Bacterial iron homeostasis. *FE* . 2003;27:215–37
17. Robin A, Vansuyt G, Hinsinger P. . Iron dynamics in the rhizosphere: consequences for plant health and nutrition. In: *A A* da15.

28. Gu S, Shao Z, Qu Z. . Siderophore-receptor coevolution analysis reveals habitat- and pathogen-specific bacterial iron interaction networks. . 2023
29. Kramer J, Ozkaya O, Kumme[redacted] R. Bacterial siderophores in community and host interactions. . 2020;18:152–63
30. Stubbendieck RM, Vargas-Bautista C, Straight PD. Bacterial communities: interactions to scale. *F* . 2016;7:1234
31. Li M, Wei Z, Wang J. . Facilitation promotes invasions in plant-associated microbial communities. *E* *L* . 2019;22:149–58
32. de los Santos-Villalobos S, Barrera-Galicia GC, Miranda-Salcedo MA. . *B* XXVI siderophore with biocontrol capacity against *C* . *J* *B* . 2012;28:2615–23
33. Yu X, Ai C, Xin L. . The siderophore-producing bacterium, *B* CAS15, has a biocontrol effect on *F* wilt and promotes the growth of pepper. *E* *J* *B* . 2011;47:138–45
34. Gu S, Yang T, Shao Z. . Siderophore-mediated interactions determine the disease suppressiveness of microbial consortia. . 2020;5:e00811–9
35. Haas D, Keel C. Regulation of antibiotic production in root-colonizing spp. and relevance for biological control of plant disease. *A* . 2003;41:117–53
36. Hu J, Wei Z, Friman VP. . Probiotic diversity enhances rhizosphere microbiome function and plant disease suppression. *B* . 2016;7:1110–28
37. Butaite E, Baumgartner M, Wyder S. . Siderophore cheating and cheating resistance shape com[redacted]tition for iron in soil and freshwater communities. *C* . 2017;8:414
38. Höfte M, Buysens S, Koedam N. . Zinc affects siderophore-mediated high affinity iron uptake systems in the rhizosphere 7NSK2. *B* . 1993;6:85–91
39. Zhou T, Chen D, Li C. . Isolation and characterization of J12 as an antagonist against and identification of its antimicrobial components. . 2012;167:388–94
40. Jousset A, Bonkowski M. The model predator *A* induces the production of 2,4,DAPG by the biocontrol strain Q2-87. *B* *B* . 2010;42:1647–9
41. Peng J, Chen G, Xu X. . Iron facilitates the RetS-Gac-Rsm cascade to inversely regulate protease IV (piv) expression via the sigma factor PvdS in . *E* . 2020;22:5402–13
42. Sindhu SS, Rakshiya YS, Sahu G. Biological control of soilborne plant pathogens with rhizosphere bacteria. . 2009;3:10–21
43. Santoyo G, Guzmán-Guzmán P, Parra-Cota FI. . Plant growth stimulation by microbial consortia. *A* . 2021;11:219
44. West SA, Buckling A. Cooperation, virulence and siderophore production in bacterial parasites. *B* . 2003;270:37–44
45. Joshi F, Archana G, Desai A. Siderophore cross-utilization amongst rhizospheric bacteria and the role of their differential affinities for Fe^{3+} on growth stimulation under iron-limited conditions. *C* . 2006;53:141–7
46. Hibbing ME, Fuqua C, Parsek MR. . Bac[redacted]rial competition: surviving and thriving in the microbial jungle. . 2010;8:15–25
47. Sheng MM, Jia HK, Zhang GY. . Siderophore production by

...0004Tc[(.)-240.6su7206;)]TJ/F11Tf3.01920TD1993